

Electromagnetic Scattering by Approximately Cloaked Dielectric Cylinder

Hany M. Zamel^{1,*}, Essam El Diwany¹, and Hadia El Hennawy²

Abstract—In cloaking, a body is hidden from detection by surrounding it by a coating consisting of an unusual anisotropic nonhomogeneous material. The permittivity and permeability of such a cloak are determined by the coordinate transformation of compressing a hidden 2D or cylindrical body into a line. Some components of the electrical parameters of the cloaking material (ε, μ) are required to have infinite or zero value at the boundary of the hidden object. In order to eliminate the zero or infinite values of the electrical parameters, approximate cloaking can be used by transforming the cylindrical body virtually into a small cylinder rather than a line, but this produces some scattering. The solution is obtained by rigorously solving Maxwell equations using angular harmonics expansion. In this work, the scattering pattern, and the backscattering cross section against the frequency for cloaked dielectric cylinder are studied for both transverse magnetic (TM_z) and transverse electric (TE_z) polarizations of the incident plane wave for different transformed body radii.

1. INTRODUCTION

Recently, the concept of electromagnetic cloaking has drawn considerable attention concerning theoretical, numerical and experimental aspects [1–7]. One approach to achieve electromagnetic cloaking is to deflect the rays that would have struck the object, guide them around the object, and return them to their original trajectory, thus no waves are scattered from the body [1]. In the coordinate transformation method for cloaking cylindrical bodies, the body to be hidden is transformed virtually into a line, and this transformation leads to radially nonhomogeneous profiles of anisotropic components of ε, μ in the cloaking coating. One problem for the line-transformed cloaks is that some component of the parameters (ε, μ) have singularities at the inner boundary. For cylindrical cloak, $\varepsilon_\phi, \mu_\phi$ are infinite while $\varepsilon_\rho, \mu_\rho, \varepsilon_z, \mu_z$ are zero. This requires the use of metamaterials which can produce such values, however, they are narrow band since they rely on using array of resonant elements (as split ring resonators) [8–11]. To avoid the problem of the infinite or zero material parameters at the hidden body boundary, two approaches have been studied. The first is removing a thin layer from the inner boundary; however, cloaking is very sensitive to this removal [12, 13]. Another technique is the use of approximate cloaking by transforming the hidden body virtually into a small object rather than a line, as shown in Fig. 1 [14–20], and for general finite cylindrical shapes [21], however, this leads to some scattering. The analysis of this technique shows that certain resonances result due to the transformed small object, a lossy layer can be used to solve this problem [15, 22, 23]. Approximate cloaking with lossy layer can be used to hide both passive bodies and active sources for electromagnetic scattering [15, 22, 23], and also for acoustic scattering [24]. Special coatings can also be used to enhance cloaking for systems governed by Helmholtz equation [25, 26].

In this work, the scattering properties of approximately cloaked dielectric cylinder are studied for both TE_z and TM_z polarizations as a function of the transformed object radius.

Received 18 January 2014, Accepted 14 March 2014, Scheduled 19 March 2014

* Corresponding author: Hany Mahmoud Zamel (res_ass@yahoo.com).

¹ Microwave Engineering Department, Electronics Research Institute, Egypt. ² Faculty of Engineering, Ain Shams University, Egypt.

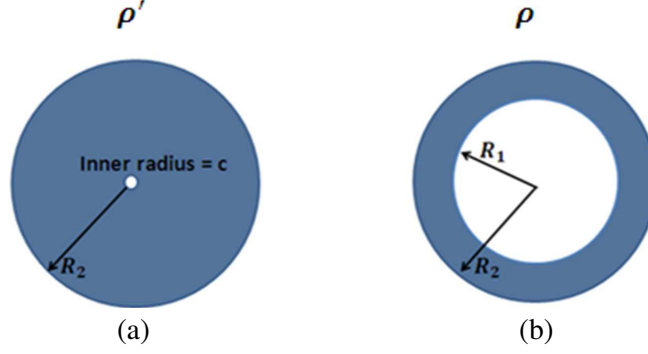


Figure 1. (a) Virtual domain, (b) actual domain.

2. COORDINATE TRANSFORMATION METHOD FOR CLOAKING — MATERIAL PARAMETERS OF THE APPROXIMATE CYLINDRICAL CLOAK

Perfect cylindrical cloak can be constructed by compressing the electromagnetic fields in a cylindrical region $\rho' \leq R_2$ into a cylindrical shell $R_1 \leq \rho \leq R_2$ as shown in Fig. 1. The coordinate transformation relates the radius ρ' in the virtual domain to the corresponding radius ρ in the cloaking material. The coordinate transformation is $\rho' = f(\rho)$, with $f(R_1) = 0$ for perfect cloaking or $f(R_1) = c$ for approximate cloaking and $f(R_2) = R_2$ [15], while φ and z are kept unchanged, where c is the reduced radius in the virtual domain. In the principal directions (ρ, φ, z in cylindrical coordinates) this transformation leads to a diagonal Jacobian matrix T [27, 28],

$$T = \begin{bmatrix} Q_\rho & 0 & 0 \\ 0 & Q_\varphi & 0 \\ 0 & 0 & Q_z \end{bmatrix} \quad (1)$$

whose elements are the stretching ratios (Q_ρ, Q_φ, Q_z) of the line elements in the principal directions ($\frac{d\rho'}{d\rho}, \frac{\rho'd\varphi'}{\rho d\varphi}, \frac{dz'}{dz}$ in the cylindrical coordinates) in the virtual domain relative to the actual domain.

The radial and transverse permittivity and permeability of the cylindrical cloak, depending on ρ , are given as [1, 29]:

$$\frac{\varepsilon_\rho}{\varepsilon_0} = \frac{\mu_\rho}{\mu_0} = \frac{Q_\varphi Q_z}{Q_\rho} = \frac{f(\rho)}{\rho f'(\rho)}, \quad \frac{\varepsilon_\varphi}{\varepsilon_0} = \frac{\mu_\varphi}{\mu_0} = \frac{Q_\rho Q_z}{Q_\varphi} = \frac{\rho f'(\rho)}{f(\rho)}, \quad \frac{\varepsilon_z}{\varepsilon_0} = \frac{\mu_z}{\mu_0} = \frac{Q_\varphi Q_\rho}{Q_z} = \frac{f(\rho) f'(\rho)}{\rho} \quad (2)$$

ε_ρ and ε_φ are reciprocals to each other.

A linear transformation is usually used, given for approximate cloaking by (for ideal cloaking $c = 0$) [15, 30]:

$$f(\rho) = \rho' = \frac{1}{(R_2 - R_1)} [\rho(R_2 - c) + R_2(c - R_1)] \quad (3)$$

Thus, the permittivity and permeability of the approximate cylindrical cloak are given from the above equations by:

$$\frac{\varepsilon_\rho}{\varepsilon_0} = \frac{\mu_\rho}{\mu_0} = \frac{\rho(R_2 - c) + R_2(c - R_1)}{\rho(R_2 - c)} \quad (4)$$

$$\frac{\varepsilon_\varphi}{\varepsilon_0} = \frac{\mu_\varphi}{\mu_0} = \frac{\rho(R_2 - c)}{\rho(R_2 - c) + R_2(c - R_1)} \quad (5)$$

$$\frac{\varepsilon_z}{\varepsilon_0} = \frac{\mu_z}{\mu_0} = \frac{\rho(R_2 - c)^2 + R_2(c - R_1)(R_2 - c)}{\rho(R_2 - R_1)^2} \quad (6)$$

At $\rho = R_1$:

$$\frac{\varepsilon_\rho}{\varepsilon_0} = \frac{R_1(R_2 - c) + R_2(c - R_1)}{R_1(R_2 - c)} = \frac{c(R_2 - R_1)}{R_1(R_2 - c)} \quad (7)$$

$$\frac{\varepsilon_\varphi}{\varepsilon_0} = \frac{R_1(R_2-c)}{R_1(R_2-c)+R_2(c-R_1)} = \frac{R_1(R_2-c)}{c(R_2-R_1)} \quad (8)$$

$$\frac{\varepsilon_z}{\varepsilon_0} = \frac{R_1(R_2-c)^2 + R_2(c-R_1)(R_2-c)}{R_1(R_2-R_1)^2} = \frac{c(R_2-c)}{R_1(R_2-R_1)} \quad (9)$$

For approximate cloaking $\varepsilon_\varphi, \mu_\varphi$ are proportional to $\frac{1}{c}$ at $\rho = R_1$, while $\varepsilon_\rho, \mu_\rho, \varepsilon_z, \mu_z$ are proportional to c . Thus, for ideal cloaking ($c = 0$), at the inner boundary, $\varepsilon_\varphi, \mu_\varphi$ are infinitely large, and the other components are zero.

At $\rho = R_2$,

$$\frac{\varepsilon_\rho}{\varepsilon_0} = \frac{R_2 - R_1}{R_2 - c} \quad (10)$$

$$\frac{\varepsilon_\varphi}{\varepsilon_0} = \frac{(R_2-c)}{(R_2-R_1)} \quad (11)$$

$$\frac{\varepsilon_z}{\varepsilon_0} = \frac{(R_2-c)^2 + (c-R_1)(R_2-c)}{(R_2-R_1)^2} = \frac{(R_2-c)}{(R_2-R_1)} \quad (12)$$

3. FORMULATION OF THE PROBLEM OF SCATTERING BY A CLOAKED CYLINDER WITH NONHOMOGENEOUS ANISOTROPIC CLOAK MATERIAL

To study the problem of scattering of a plane EM wave by a cloaked dielectric cylinder, the fields are expanded in cylindrical harmonics in the different regions (as will be shown) in the actual domain (air, cloaking shell and dielectric), and the boundary conditions are applied at the interfaces. For normally incident wave on the cylinder, Maxwell's equations can be decomposed into TE_z (E_ρ, E_φ, H_z) and TM_z (H_ρ, H_φ, E_z) fields w.r.t the axial \hat{z} direction. Thus, for TE_z fields only μ_z, ε_ρ and ε_φ are required when analyzing scattering. TM_z fields require ε_z, μ_ρ and μ_φ .

3.1. The Differential Equation for the Axial Field Component in the Cloak Region

Maxwell's equations for TM_z polarization are [31]:

$$E_z = \frac{1}{j\omega\varepsilon_z\rho} \left[\frac{\partial(\rho H_\varphi)}{\partial\rho} - \frac{\partial H_\rho}{\partial\varphi} \right] \quad (13)$$

$$H_\rho = -\frac{1}{j\omega\mu_\rho\rho} \frac{\partial E_z}{\partial\varphi} \quad (14)$$

$$H_\varphi = \frac{1}{j\omega\mu_\varphi} \frac{\partial E_z}{\partial\rho} \quad (15)$$

where ω is the angular frequency, $j = \sqrt{-1}$. The general wave equation governing the behavior of TM_z fields within a radially nonhomogeneous anisotropic material can be developed by substituting Eqs. (14) and (15) into Eq. (13).

$$E_z = \frac{1}{j\omega\varepsilon_z\rho} \left[\frac{\partial}{\partial\rho} \left(\frac{\rho}{j\omega\mu_\varphi} \frac{\partial E_z}{\partial\rho} \right) - \frac{\partial}{\partial\varphi} \left(-\frac{1}{j\omega\mu_\rho\rho} \frac{\partial E_z}{\partial\varphi} \right) \right] \quad (16)$$

Eq. (16) can be rewritten as [31]:

$$\frac{1}{\left(\frac{\varepsilon_z}{\varepsilon_0}\right)\rho} \left[\frac{\partial}{\partial\rho} \left(\frac{\rho}{\left(\frac{\mu_\varphi}{\mu_0}\right)} \frac{\partial E_z}{\partial\rho} \right) \right] + \frac{1}{\left(\frac{\varepsilon_z}{\varepsilon_0}\right)\rho^2} \frac{\partial}{\partial\varphi} \left(\frac{1}{\left(\frac{\mu_\rho}{\mu_0}\right)} \frac{\partial E_z}{\partial\varphi} \right) + k_0^2 E_z = 0 \quad (17)$$

where k_0 is the free-space wave number, $k_0 = \omega\sqrt{\mu_0\varepsilon_0}$. By substituting from Eq. (2) into Eq. (17), we get:

$$\frac{1}{f(\rho)} \frac{\partial}{\partial f} \left(f(\rho) \frac{\partial E_z}{\partial f} \right) + \frac{1}{f^2(\rho)} \frac{\partial}{\partial\varphi} \left(\frac{\partial E_z}{\partial\varphi} \right) + k_0^2 E_z = 0 \quad (18)$$

Therefore, a suitable solution of the above equation can be expressed as [32]:

$$E_z = \left[F_n J_n(k_0 f(\rho)) + C_n H_n^{(2)}(k_0 f(\rho)) \right] e^{jn\varphi} \quad (19)$$

where J_n is the n th order Bessel function of the first kind, n is integer, and $H_n^{(2)}$ is the n th order Hankel function of the second kind.

This means that the solution in the actual domain at a radius ρ is obtained in terms of Bessel functions with argument corresponding to the virtual domain at the transformed radius $f(\rho)$.

3.2. The Field Expansions and Application of Boundary Conditions

Figure 2 shows an E_z polarized plane wave with amplitude E_0 , $E^i = E_0 e^{-jk_0 x} \hat{z}$, incident upon the coated dielectric cylinder along the \hat{x} direction. The time dependence of $e^{j\omega t}$ is suppressed.

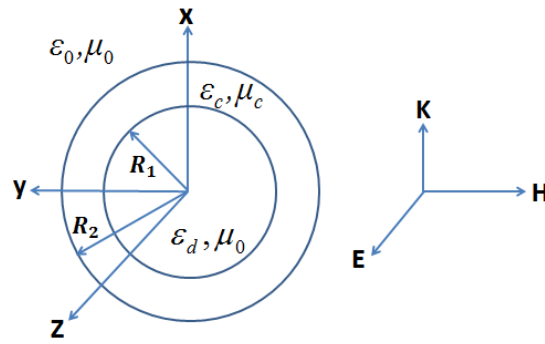


Figure 2. Configuration of scattering of a plane wave by a coated cylinder.

In order to apply the boundary conditions at the cylindrical surfaces, the fields in the different regions are expanded in terms of cylindrical wave functions with unknown coefficients.

3.2.1. The TM_z Case

For a TM_z polarized incident plane wave, the incident field can be expressed in terms of cylindrical waves [33, 34]:

$$E_z^{inc} = e^{-jk_0 x} E_0 = E_0 \sum_{n=-\infty}^{\infty} (j)^{-n} J_n(k_0 \rho) e^{jn\varphi} \quad \rho > R_2 \quad (20)$$

The scattered field can be expressed as [33, 34]:

$$E_z^s = E_0 \sum_{n=-\infty}^{\infty} (j)^{-n} A_n H_n^{(2)}(k_0 \rho) e^{jn\varphi} \quad \rho > R_2 \quad (21)$$

where the scattered field is expressed using the cylindrical Hankel function $H_n^{(2)}(k_0 \rho)$ representing scattered outgoing waves.

As shown in Eq. (19), the field inside the cloak region can be expressed as:

$$E_z^c = E_0 \sum_{n=-\infty}^{\infty} \left[F_n J_n(k_0 f(\rho)) + C_n H_n^{(2)}(k_0 f(\rho)) \right] e^{jn\varphi} \quad R_1 < \rho < R_2 \quad (22)$$

where the fields in the cloak region are represented by Bessel and Hankel functions of argument $(k_0 f(\rho))$. The expansion in the dielectric region is:

$$E^d = \sum_{n=-\infty}^{\infty} D_n J_n(k_d \rho) e^{jn\varphi} \quad \rho < R_1 \quad (23)$$

where k_d is the wave number in the dielectric region, $k_d = \omega \sqrt{\mu_0 \epsilon_d}$.

The boundary conditions are that the tangential components E_z and H_φ are continuous across the cylindrical interfaces $\rho = R_1$ and R_2 . At $\rho = R_2$, the tangential electric field components E_z give:

$$[E_z^{inc} + E_z^s]_{\rho=R_2} = [E_z^c]_{\rho=R_2}$$

$$(j)^{-n} J_n(k_0 R_2) + (j)^{-n} A_n H_n^{(2)}(k_0 R_2) = F_n J_n(k_0 R_2) + C_n H_n^{(2)}(k_0 R_2) \quad (24)$$

The boundary condition for H_φ is :

$$[H_\varphi^{inc} + H_\varphi^s]_{\rho=R_2} = [H_\varphi^c]_{\rho=R_2},$$

where H_φ is obtained from Eq. (15). Thus:

$$\frac{k_0}{j\mu_0\omega} (j)^{-n} [J_n(k_0 R_2)]' + \frac{k_0}{j\mu_0\omega} (j)^{-n} A_n [H_n^{(2)}(k_0 R_2)]' = \frac{k_0}{j\mu_\varphi\omega} \left[\begin{array}{l} F_n [J_n(k_0 R_2)]' \\ + C_n [H_n^{(2)}(k_0 R_2)]' \end{array} \right] \frac{df(\rho)}{d\rho} \Big|_{\rho=R_2} \quad (25)$$

where $\mu_\varphi = \mu_0 \frac{\rho}{f(\rho)} \frac{df(\rho)}{d\rho}$, Eq. (2), and $f(R_2) = R_2$. The primes at the square brackets indicate differentiation with respect to the argument $k_0\rho$. Thus Eq. (25) becomes:

$$\frac{k_0}{j\mu_0\omega} (j)^{-n} \left[[J_n(k_0 R_2)]' + A_n [H_n^{(2)}(k_0 R_2)]' \right] = \frac{k_0}{j\mu_0\omega} \left[\begin{array}{l} F_n [J_n(k_0 R_2)]' \\ + C_n [H_n^{(2)}(k_0 R_2)]' \end{array} \right] \quad (26)$$

Eqs. (24) and (26) lead to:

$$F_n = (j)^{-n}, \quad C_n = (j)^{-n} A_n \quad (27)$$

Similar conditions are applied at $\rho = R_1$, which corresponds to $\rho' = c$ in the cloak region, thus we have:

$$[E_z^c]_{\rho=R_1} = [E_z^d]_{\rho=R_1}, \quad F_n J_n(k_0 c) + C_n H_n^{(2)}(k_0 c) = D_n J_n(k_d R_1) \quad (28)$$

$$[H_\varphi^c]_{\rho=R_1} = [H_\varphi^d]_{\rho=R_1}, \quad \frac{k_0}{j\mu_\varphi\omega} \left[F_n [J_n(k_0 c)]' + C_n [H_n^{(2)}(k_0 c)]' \right] \frac{df(\rho)}{d\rho} \Big|_{\rho=R_1} = \frac{k_d}{j\mu_0\omega} [D_n [J_n(k_d R_1)]'] \quad (29)$$

By substituting for μ_φ from Eq. (2) into Eq. (29), then

$$\frac{\eta_o c}{R_1} \left[F_n [J_n(k_0 c)]' + C_n [H_n^{(2)}(k_0 c)]' \right] = \frac{1}{\eta_d} [D_n [J_n(k_d R_1)]'] \quad (30)$$

where $\eta_o = \sqrt{\frac{\mu_0}{\epsilon_0}}$ and $\eta_d = \sqrt{\frac{\mu_0}{\epsilon_d}}$.

By substituting Eq. (27) into Eqs. (28), (30), we get the scattering coefficient A_n (TM_z case):

$$A_n = - \left[\frac{c\eta_d J_n(k_d R_1) [J_n(k_0 c)]' - R_1 \eta_o J_n(k_0 c) [J_n(k_d R_1)]'}{c\eta_d J_n(k_d R_1) [H_n^{(2)}(k_0 c)]' - R_1 \eta_o H_n^{(2)}(k_0 c) [J_n(k_d R_1)]'} \right] \quad (31)$$

3.2.2. The TE_z Case

The scattering for the TE_z case can be obtained by the procedure used above. The incident field H_z^{inc} is given by Eq. (20) by replacing E_0 by H_0 . The scattering coefficient A_n in Eq. (21) is replaced by \tilde{B}_n . The coefficients F_n, C_n in Eq. (22) are replaced by P_n, S_n , respectively. The coefficient D_n in Eq. (23) is replaced by E_n .

At $\rho = R_2$, the continuity of the tangential magnetic field components H_z gives:

$$[H_z^i + H_z^s]_{\rho=R_2} = [H_z^c]_{\rho=R_2}, \quad (j)^{-n} J_n(k_0 R_2) + (j)^{-n} B_n H_n^{(2)}(k_0 R_2) = P_n J_n(k_0 R_2) + S_n H_n^{(2)}(k_0 R_2) \quad (32)$$

From Maxwell equation, E_φ is given by:

$$E_\varphi = \frac{-1}{j\omega\epsilon_\varphi} \frac{\partial H_z}{\partial \rho} \quad (33)$$

The boundary condition for E_φ is:

$$[E_\varphi^i + E_\varphi^s]_{\rho=R_2} = [E_\varphi^c]_{\rho=R_2}$$

$$\frac{-k_0}{j\varepsilon_0\omega} (j)^{-n} \left[[J_n(k_0R_2)]' + B_n [H_n^{(2)}(k_0R_2)]' \right] = \left[\frac{-k_0}{j\varepsilon_\varphi\omega} \left[\begin{array}{c} P_n [J_n(k_0R_2)]' \\ + S_n [H_n^{(2)}(k_0R_2)]' \end{array} \right] \frac{df(\rho)}{d\rho} \right]_{\rho=R_2} \quad (34)$$

where $\varepsilon_\varphi = \varepsilon_0 \frac{\rho}{f(\rho)} \frac{df(\rho)}{d\rho}$. Thus,

$$(j)^{-n} \left[[J_n(k_0R_2)]' + B_n [H_n^{(2)}(k_0R_2)]' \right] = \left[P_n [J_n(k_0R_2)]' + S_n [H_n^{(2)}(k_0R_2)]' \right] \quad (35)$$

Eqs. (32) and (35) lead to:

$$P_n = (j)^{-n}, \quad S_n = (j)^{-n} B_n \quad (36)$$

Similar conditions are applied at $\rho = R_1$, which corresponds to $\rho' = c$ in the cloak region, thus we have:

$$[H_z^c]_{\rho=R_1} = [H_z^d]_{\rho=R_1}, \quad (j)^{-n} J_n(k_0c) + (j)^{-n} B_n H_n^{(2)}(k_0c) = E_n J_n(k_d R_1) \quad (37)$$

$$[E_\varphi^c]_{\rho=R_1} = [E_\varphi^d]_{\rho=R_1},$$

$$\frac{-k_0}{j\varepsilon_\varphi\omega} \left[(j)^{-n} [J_n(k_0c)]' + (j)^{-n} B_n [H_n^{(2)}(k_0c)]' \right] \frac{df(\rho)}{d\rho} \Big|_{\rho=R_1} = \frac{-k_d}{j\varepsilon_d\omega} [E_n [J_n(k_d R_1)]'] \quad (38)$$

By substituting ε_φ in Eq. (38), then

$$\frac{\eta_0 c}{R_1} \left[(j)^{-n} [J_n(k_0c)]' + (j)^{-n} B_n [H_n^{(2)}(k_0c)]' \right] = \eta_d [E_n [J_n(k_0 R_1)]'] \quad (39)$$

By solving Eqs. (37), (39), we get the scattering coefficient B_n (TE_z case):

$$B_n = - \left[\frac{c\eta_0 J_n(k_d R_1) [J_n(k_0c)]' - R_1 \eta_d J_n(k_0c) [J_n(k_d R_1)]'}{c\eta_0 J_n(k_d R_1) [H_n^{(2)}(k_0c)]' - R_1 \eta_d H_n^{(2)}(k_0c) [J_n(k_d R_1)]'} \right] \quad (40)$$

in agreement with [16, 19, 20] that the scattering from the cloaked body is equivalent to that produced by the body of reduced size with the values of ε , μ modified using a linear transformation for the region of the hidden body.

It is to be noted that A_n and B_n are independent of the outer radius R_2 . The difference between the two expressions is in exchanging η_0 and η_d . The expressions for A_n and B_n can lead to resonance behavior [15, 18].

For $c = R_1$, these coefficients are the same as the solution for scattering by a dielectric cylinder [34, 35]. The mode series is truncated at the mode number $n_{\max} = k_0 R_2 + 5$ [36].

4. THE SCATTERING WIDTH

For the 2-D scattering problem, the scattering width $\sigma(\varphi)$, which is referred to as the scattering cross section per unit length, is defined as [35]:

$$\sigma(\varphi) = \lim_{\rho \rightarrow \infty} 2\pi\rho \frac{|E^s(\varphi)|^2}{|E^i|^2} = \lim_{\rho \rightarrow \infty} 2\pi\rho \frac{|H^s(\varphi)|^2}{|H^i|^2} \quad (41)$$

The scattering width $\sigma(\varphi)$ defines the scattering in an arbitrary direction (for forward scattering $\varphi = 0^\circ$, for backscattering $\varphi = \pi$).

For TM_z case [35]:

$$\sigma(\varphi) = \frac{4}{k_0} \left| \sum_{n=0}^{\infty} (-1)^n \epsilon_n A_n \cos(n\varphi) \right|^2 \quad (42)$$

For TE_z case [35]:

$$\sigma(\varphi) = \frac{4}{k_0} \left| \sum_{n=0}^{\infty} (-1)^n \epsilon_n B_n \cos(n\varphi) \right|^2 \quad (43)$$

where the Neuman number $\epsilon_n = \begin{cases} 1, & \text{for } n = 0 \\ 2, & \text{for } n = 1, 2, 3, \dots \end{cases}$.

5. LOW FREQUENCY ASYMPTOTIC SCATTERING

For electrically small dielectric cylinder with $k_d R_1 \ll 1$ and $k_0 c \ll 1$, an approximate solution can be obtained by keeping only the first terms of the field expansions by using the small — argument approximations [37]:

$$\begin{aligned} J_0(z) &\cong 1, & H_0^{(2)}(z) &\cong 1 - \frac{2j}{\pi} \left(\ln \frac{z}{2} + 0.5772 \right), & J_0'(z) &\cong \frac{-z}{2}, & \frac{d}{dz} H_0^{(2)}(z) &\cong \frac{-2j}{\pi z}, & J_1(z) &\cong \frac{z}{2}, \\ H_1^{(2)}(z) &\cong \frac{-2j}{\pi z}, & J_1'(z) &\cong \frac{1}{2}, & \frac{d}{dz} H_1^{(2)}(z) &\cong \frac{-2j}{\pi z^2}, & & & & \text{when } z \rightarrow 0 \end{aligned} \quad (44)$$

5.1. Scattering Widths for Cloaked Dielectric Cylinder

The coefficients for the first terms of the dielectric cylinder, Eqs. (31), (40), are found as:

$$A_0 \approx \frac{\frac{k_0}{2} (R_1^2 \varepsilon_r - c^2)}{\frac{2j}{\pi k_0} - \frac{k_0}{2} R_1^2 \varepsilon_r \left(1 - \frac{2j}{\pi} \ln(0.8905 k_0 c) \right)}, \quad (\varepsilon_r = \varepsilon_d / \varepsilon_0) \quad (45)$$

For $R_1^2 \varepsilon_r \gg c^2$

$$A_0 \approx \frac{-1}{1 - \frac{2j}{\pi} \left(\frac{2}{k_0^2 R_1^2 \varepsilon_r} + \ln(0.8905 k_0 c) \right)} \quad (46)$$

Also:

$$B_0 \approx \frac{-\frac{k_0}{2} (R_1^2 - c^2)}{\frac{-2j}{\pi k_0} + \frac{k_0}{2} R_1^2 \varepsilon_r \left(1 - \frac{2j}{\pi} \ln(0.8905 k_0 c) \right)} \quad (47)$$

For $R_1^2 \gg c^2$

$$B_0 \approx \frac{-1}{1 - \frac{2j}{\pi} \left(\frac{2}{k_0^2 R_1^2} + \ln(0.8905 k_0 c) \right)} \quad (48)$$

Also:

$$B_1 \approx \frac{k_0^2 c^2 \pi \varepsilon_r - 1}{4j \varepsilon_r + 1} \ll B_0 \quad (49)$$

Thus, the backscattering widths are given by:

$$\sigma(\varphi = \pi) \cong \frac{4}{k_0} \frac{1}{1 + \frac{4}{\pi^2} \left(\frac{2}{k_0^2 R_1^2 \varepsilon_r} + \ln(0.8905 k_0 c) \right)^2} \quad (\text{TM}_z \text{ case}) \quad (50)$$

$$\sigma(\varphi = \pi) \cong \frac{4}{k_0} \frac{1}{1 + \frac{4}{\pi^2} \left(\frac{2}{k_0^2 R_1^2} + \ln(0.8905 k_0 c) \right)^2} \quad (\text{TE}_z \text{ case}) \quad (51)$$

We can conclude that, the effect of c is small on the behaviour of the scattering width for TE_z and TM_z cases for the dielectric cylinder at low frequencies.

6. RESULTS

Normalized bistatic scattering pattern and backscattering versus frequency are studied with $R_2 = 2R_1$. For the bistatic scattering $R_1 = \lambda$.

6.1. Scattering by a Cloaked Dielectric Cylinder

For scattering by a cloaked dielectric cylinder, we consider cylinders with relative permittivities of 4 and 8. Figs. 3, 4 show the normalized bistatic scattering width (σ/R_1) for a cloaked circular dielectric cylinder versus φ with a relative permittivity of 4 with three different radii c for TE_z and TM_z cases, respectively. The scattering decreases as c decreases. The scattering from the cloaked cylinder in certain directions may be higher than the scattering from the dielectric cylinder at the angles where the latter scattering is low.

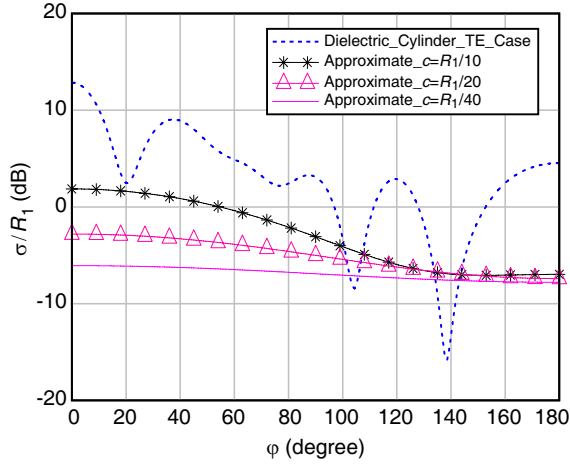


Figure 3. Normalized bistatic scattering width for a cloaked circular dielectric cylinder, $\varepsilon_r = 4$ (TE_z case).

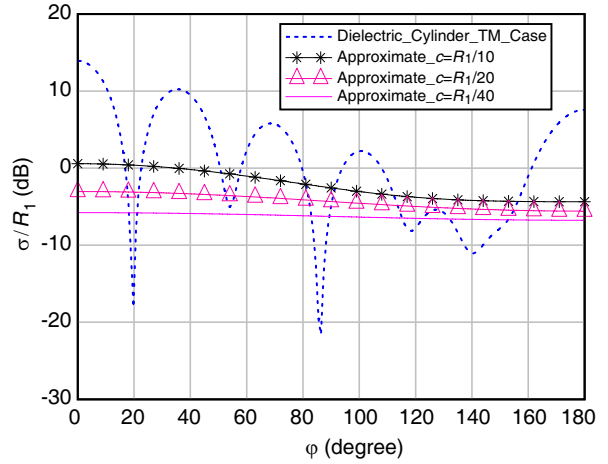


Figure 4. Normalized bistatic scattering width for a cloaked circular dielectric cylinder, $\varepsilon_r = 4$ (TM_z case).

Figures 5, 6 show the normalized backscattering width ($\sigma/\pi R_1$) for a circular dielectric cylinder versus the normalized frequency $k_0 R_1$ with a relative permittivity of 4 with three different radii c for TE_z and TM_z cases, respectively. At higher frequencies the scattering decreases as c decreases. The cloaked dielectric cylinder produces larger scattering than the uncloaked cylinder in a range of low frequencies.

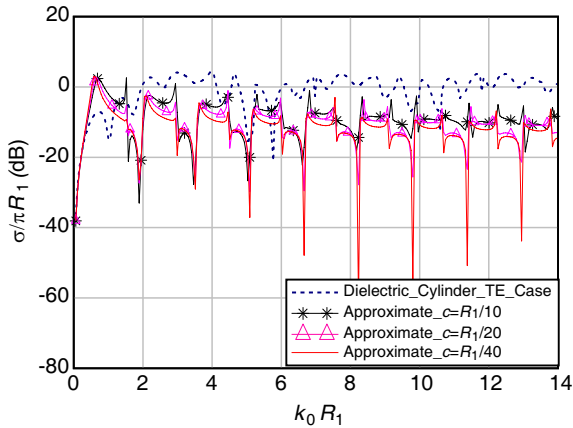


Figure 5. Normalized backscattering width for a cloaked circular dielectric cylinder, $\varepsilon_r = 4$ (TE_z case).

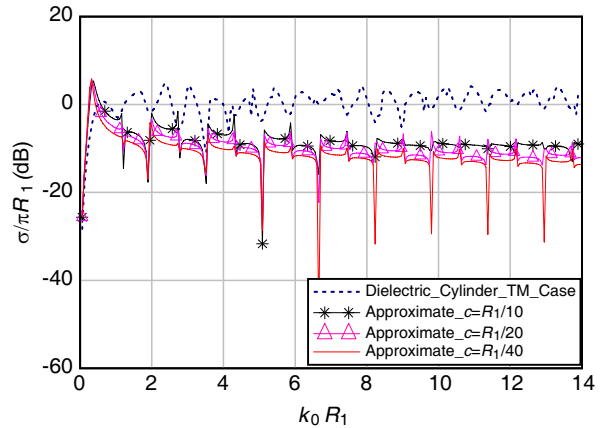


Figure 6. Normalized backscattering width for a cloaked circular dielectric cylinder, $\varepsilon_r = 4$ (TM_z case).

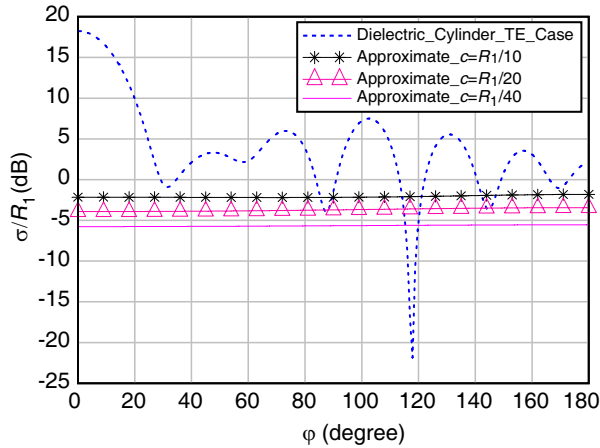


Figure 7. Normalized bistatic scattering width for a cloaked circular dielectric cylinder, $\epsilon_r = 8$ (TE_z case).

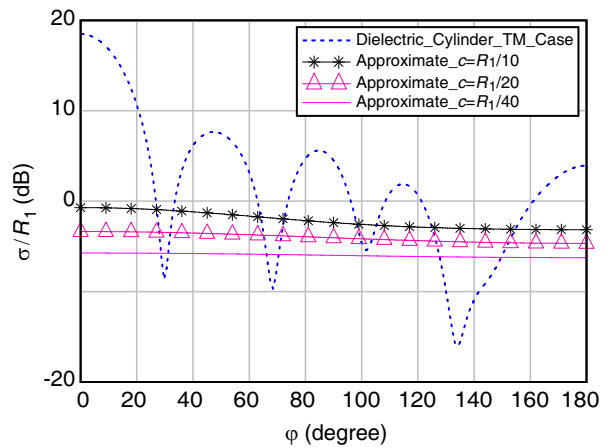


Figure 8. Normalized bistatic scattering width for a cloaked circular dielectric cylinder, $\epsilon_r = 8$ (TM_z case).

Figures 7, 8 show the normalized bistatic scattering width (σ/R_1) for a circular dielectric cylinder versus φ with a relative permittivity of 8 with three different radii c for TE_z and TM_z cases, respectively. From Figs. 7, 8, we can conclude that the normalized bistatic scattering width is nearly constant with increasing φ for different values of c for the used operating dimensions.

Figures 9, 10 show the normalized backscattering width ($\sigma/\pi R_1$) for a circular dielectric cylinder versus $k_0 R_1$ with a relative permittivity of 8 with three different radii c for TE_z and TM_z cases, respectively. The scattering behavior is similar to that for $\epsilon_r = 4$, except that the number of resonances increases as the relative permittivity increases.

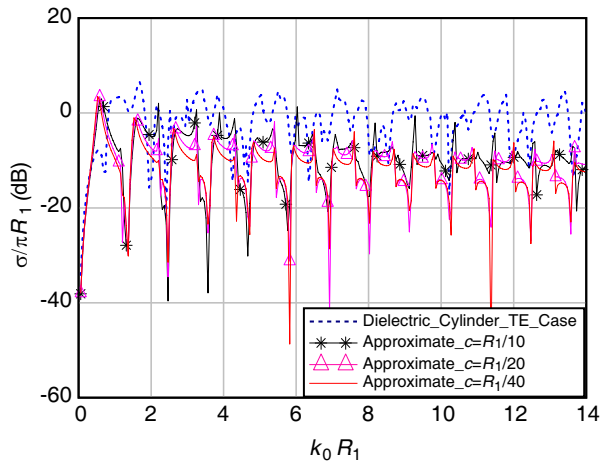


Figure 9. Normalized backscattering width for a cloaked circular dielectric cylinder, $\epsilon_r = 8$ (TE_z case).

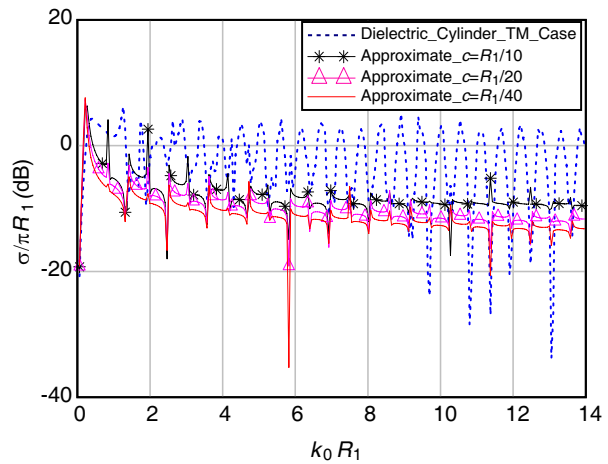


Figure 10. Normalized backscattering width for a cloaked circular dielectric cylinder, $\epsilon_r = 8$ (TM_z case).

6.2. Permittivity and Permeability Profiles in the Cloak Region

Figures 11–13 show the values of the material parameters in the cloaking material for perfect cloaking ($c = 0$) and two different radii for approximate cloaks, Eqs. (4)–(6), with $R_2 = 2R_1$. For the ideal case, the value of the relative permittivity ϵ_φ at the inner boundary approaches infinity, Eq. (8), but for

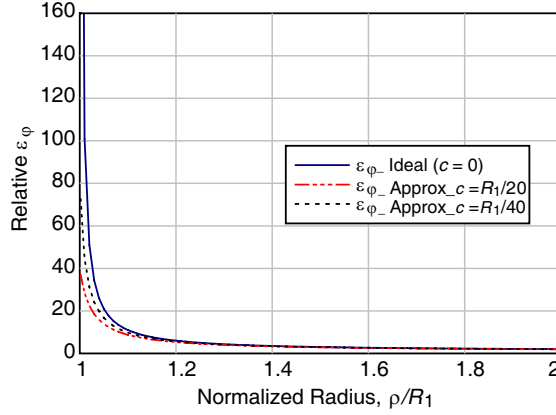


Figure 11. Relative permittivity component ε_φ versus the radius in the cloaking region.

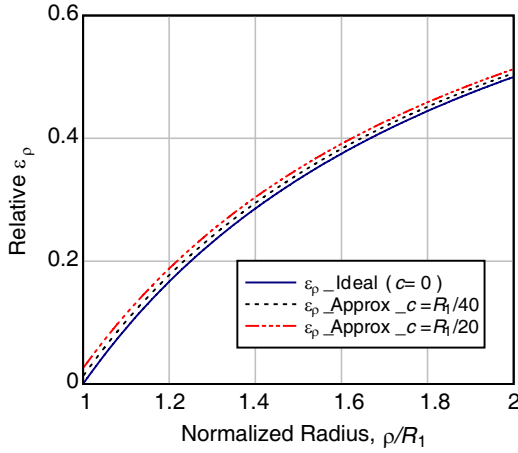


Figure 12. Relative permittivity component ε_ρ versus the radius in the cloaking region.

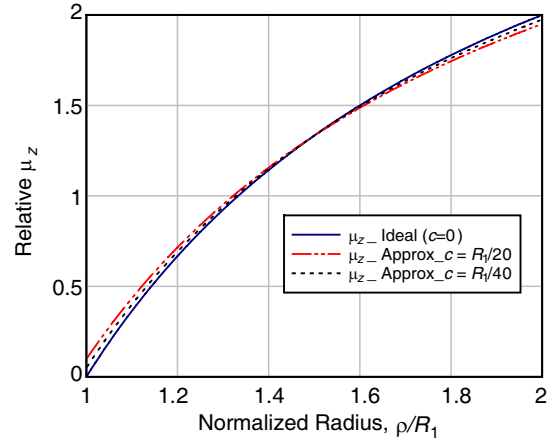


Figure 13. Relative permeability component μ_z versus the radius in the cloaking region.

approximate cloaking the value of ε_φ at the inner layer is finite (39 for $c = R_1/20$ and 79 for $c = R_1/40$), Eq. (8), as shown in Fig. 11. For ideal cloak ($c = 0$), ε_ρ is zero at the inner boundary, Eq. (7), but for approximate cloaking the value of the relative permeability ε_ρ is finite (0.026 for $c = R_1/20$ and 0.013 for $c = R_1/40$). Also, for ideal cloak ($c = 0$), μ_z is zero at the inner boundary, Eq. (9), but for approximate cloaking the value of the relative permeability μ_z is finite (0.0975 for $c = R_1/20$ and 0.0494 for $c = R_1/40$).

7. CONCLUSION

In this work, the scattering from a cloaked dielectric cylinder is studied for both TE_z and TM_z cases for anisotropic nonhomogeneous cloaking profiles. For cloaked dielectric cylinder, the scattering expressions for the TE_z and TM_z cases are the same except for exchanging η_0 and η_d . The low frequency asymptotic expressions show that the effect of c is small on the behaviour of the scattering width for TE_z and TM_z cases for the dielectric cylinder.

For a cloaked dielectric cylinder the scattering decreases as c decreases at higher frequencies. The cloaked dielectric cylinder produces larger scattering than the uncloaked cylinder in a range of low frequencies. The scattering behaviour for cloaked dielectric cylinders show resonances, with the number of resonances increasing as the relative permittivity increases.

REFERENCES

1. Pendry, J. B., D. Schurig, and D. R. Smith, "Controlling electromagnetic fields," *Science*, Vol. 312, 1780–1782, 2006.
2. Kwon, D. and D. Werner, "Transformation electromagnetics: An overview of the theory and applications," *IEEE Ant. and Prop. Mag.*, Vol. 52, No. 1, 24–46, 2010.
3. Yan, M., Z. Ruan, and M. Qiu, "Scattering characteristics of simplified cylindrical invisibility cloaks," *Opt. Exp.*, Vol. 15, No. 26, 17772–17782, 2007.
4. Alitalo, P. and S. Tretyakov, "Numerical modeling and characterization of selected electromagnetic cloaking structures," *Inter. J. of RF and Micro. Computer — Aided Eng.*, Vol. 22, No. 4, 483–495, 2012.
5. Cummer, S., B. Popa, D. Schurig, D. Smith, and J. Pendry, "Full-wave simulations of electromagnetic cloaking structures," *Phys. Rev. E*, Vol. 74, 36621-1–5, 2006.
6. Li, J., Y. Huang, and W. Yang, "Developing a time-domain finite-element method for modeling of electromagnetic cylindrical cloaks," *J. of Comp. Phys.*, Vol. 231, No. 7, 2880–2891, 2012.
7. Schurig, D., J. J. Mock, B. J. Justice, S. A. Cummer, J. B. Pendry, A. F. Starr, and D. R. Smith, "Metamaterial electromagnetic cloak at microwave frequencies," *Science*, Vol. 314, 977–980, Oct. 2006.
8. Pendry, J. B., A. J. Holden, D. J. Robbins, and W. J. Stewart, "Magnetism from conductors and enhanced nonlinear phenomena," *IEEE Transactions on Microwave Theory and Techniques*, Vol. 47, No. 11, 2075–2084, Nov. 1999.
9. Eleftheriades, G. V. and K. G. Balmain, *Negative Refraction Metamaterials — Fundamental Principles and Applications*, John Wiley, 2005.
10. Engheta, N. and R. W. Ziolkowski, *Metamaterials: Physics and Engineering Explorations*, Wiley-IEEE Press, 2006.
11. Wang, J., S. Qu, J. Zhang, H. Ma, Y. Yang, C. Gu, X. Wu, and Z. Xu, "A tunable left-handed metamaterial based on modified broadside-coupled split-ring resonators," *Progress In Electromagnetics Research Letters*, Vol. 6, 35–45, 2009.
12. Ruan, Z., M. Yan, C. W. Neff, and M. Qiu, "Ideal cylindrical cloak: Perfect but sensitive to tiny perturbations," *Phys. Rev. Lett.*, Vol. 99, 113903-1–4, 2007.
13. Shahzad, A., F. Qasim, S. Ahmed, and Q. A. Naqvi, "Cylindrical invisibility cloak incorporating PEMC at perturbed void region," *Progress In Electromagnetics Research M*, Vol. 21, 61–76, 2011.
14. Liu, H., "Virtual reshaping and invisibility in obstacle scattering," *Inverse Problems*, Vol. 25, No. 4, 1–10, 2009.
15. Zhou, T., "Electromagnetic inverse problems and cloaking," Ph. D. Thesis, Washington University, 2010.
16. Isic, G., R. Gajic, B. Novakovic, Z. V. Popovic, and K. Hingerl, "Radiation and scattering from imperfect cylindrical electromagnetic cloaks," *Opt. Exp.*, Vol. 16, 1413–1422, 2008.
17. Song, W., X. Yang, and X. Sheng, "Scattering characteristics of 2-D imperfect cloaks with layered isotropic materials," *IEEE Ant. and Propag. Let.*, Vol. 11, 53–56, 2012.
18. Kohn, R., D. Onofrei, M. Vogelius, and M. Weinstein, "Cloaking via change of variables for the Helmholtz equation," *Comm. on Pure and App. Math.*, Vol. 63, No. 8, 973–1016, 2010.
19. Tinghua, T., M. Huang, W. Li, J. Yang, and Q. Zhang, "A novel proposal for simplified design of metamaterial shrinking device," *Int. Jour. for Light and Electron. Optics*, Vol. 124, No. 21, 5232–5236, 2013.
20. Jiang, W., T. Cui, X. Yang, H. Ma, and Q. Cheng, "Shrinking an arbitrary object as one desires using metamaterials," *App. Phys. Let.*, Vol. 98, 204101-1–3, 2011.
21. Li, J. Z. and H. Y. Liu, "A class of polarization-invariant directional cloaks by concatenation via transformation optics," *Progress In Electromagnetics Research*, Vol. 123, 175–187, 2012.
22. Liu, H. Y. and T. Zhou, "On approximate electromagnetic cloaking by transformation media," *SIAM J. Appl. Math.*, Vol. 71, 218–241, 2011.

23. Bao, G., H. Y. Liu, and J. Zou, “Nearly cloaking the full Maxwell equations: Cloaking active contents with general conducting layers,” *J. Math. Pures et Appl.*, 1–18, 2013.
24. Liu, H. Y., “On near-cloak in acoustic scattering,” *J. Differential Equations*, Vol. 254, 1230–1246, 2013.
25. Liu, H. Y. and H. Sun, “Enhanced near-cloak by FSH lining,” *J. Math. Pures et Appl.*, Vol. 99, No. 1, 17–42, 2013.
26. Li, J., H. Y. Liu, and H. Sun, “Enhanced approximate cloaking by SH and FSH lining,” *Inverse Problems*, Vol. 28, No. 7, 075011-1–21, 2012.
27. McGuirk, J., “Electromagnetic field control and optimization using metamaterials,” Ph.D. Thesis, Air University, Ohio, USA, 2009.
28. Hu, J., X. Zhou, and G. Hu, “Design method for electromagnetic cloak with arbitrary shapes based on Laplace’s equation,” *Opt. Exp.*, Vol. 17, No. 15, 13070–13070, 2009.
29. Yan, M., W. Yan, and M. Qiu, “Invisibility cloaking by coordinate transformation,” *Progress in Optics*, Vol. 52, 261–304, 2009.
30. Zamel, H., E. El-Diwany, and H. El-Hennawy, “Approximate electromagnetic cloaking of spherical bodies,” *National Radio Science Conference (NRSC)*, 19–28, Egypt, 2012.
31. McGuirk, J. and P. Collins, “Controlling the transmitted field into a cylindrical cloak’s hidden region,” *Optics Express*, Vol. 16, No. 22, 17560–17573, 2008.
32. Zhang, B., “Study of transformation-based invisibility cloaks,” Ph.D. Thesis, Massachusetts, 2009.
33. Harrington, R. F., *Time Harmonic Electromagnetic Fields*, McGraw-Hill, 1961.
34. Jin, J., *Theory and Computation of Electromagnetic Fields*, John Wiley, 2010.
35. Ruck, G. T., D. E. Barrick, W. D. Stuart, and C. K. Krichbaum, *Radar Cross Section Handbook*, Kluwer Academic, 1970.
36. Li, C. and Z. Shen, “Electromagnetic scattering by a conducting cylinder coated with metamaterials,” *Progress In Electromagnetics Research*, Vol. 42, 91–105, 2003.
37. Abramowitz, M. and I. Stegun, *Handbook of Mathematical Functions*, Dover, 1965.